

Supplementary Information

Experimental section

Materials: Pristine h-BN powder was purchased from Sigma-Aldrich (USA). All oligonucleotides were purchased from TaKaRa Biotechnology (China). DNA and miRNA concentrations were estimated by measuring the absorbance at 260 nm. All other chemicals were bought from Aladdin reagent Co. Ltd. (China) with analytical grade and used as received without further purification. The ultrapure water (18.2 M Ω ·cm) used throughout all experiments was purified through a Life Sciences purification system (PALL, USA). All glassware was cleaned with fresh aqua regia (HCl/HNO₃ = 3:1, v/v) before use.

Synthesis of hexagonal boron nitride nanosheet: H-BNNS was synthesized by liquid exfoliation of pristine h-BN powders. Typically, 100 mg pristine h-BN powders were dispersed in 10 mL ethanol and exfoliated by ultrasonic cell disruptor. Then, the exfoliated solution containing pristine h-BN and h-BNNS was collected and subjected to centrifugation at 6,000 rpm for 10 min. Finally, the resulting supernatant solution containing the h-BNNS with the concentration about 0.6 mg·mL⁻¹ was collected.

Characterization of hexagonal boron nitride nanosheet: TEM measurements were performed on a HITACHI H-8100 electron microscopy (Hitachi, Japan) with an accelerating voltage of 200 kV. XPS measurements were performed on an ESCALABMK II X-ray photoelectron spectrometer using Mg as the exciting source. Fluorescent emission spectra were recorded on a Hitachi RF-6000 spectrofluorometer (Hitachi, Japan).

Performance evaluation of miRNA detection in vitro: Nanoprobes (P_{miR21}-h-BNNS complex) were prepared via the immobilization of fluorescently-labeled single-stranded DNA (ssDNA) P_{miR21} on the surface of h-BNNS nanosheets. To achieve this, the DNA probe solution (prepared in PBS) was added to nanosheets and the mixture was allowed to incubate at room temperature for 30 min. Excess DNA strands were removed by centrifugation. The volume of each sample for fluorescence measurement was 300 μ L in 0.01 M PBS. The excitation was at 480 nm and the emission was

monitored at 518 nm. The concentrations of P_{miR21} and T₁, T₂, T₃, T₄ (the complementary and base-mismatched targets) used in this study were 10 nM and 300 nM, respectively.

Oligonucleotide sequences (mismatch underlined):

(1) The FAM (fluorescein-based dye) dye-labeled ssDNA (P_{miR21}): 5'-FAM-TCA ACA TCA GTC TGA TAA GCT A-3'

(2) The complementary target to P_{miR21} (miR-21, T₁): 5'-UAG CUU AUC AGA CUG AUG UUG A-3'

(3) The single-base-mismatched target to P_{miR21} (T₂): 5'-UAC C CUU AUC AGA CUG AUG UUG A-3'

(4) The two-base-mismatched target to P_{miR21} (T₃): 5'-UAC C CUU AUC AGA CUG AUG CUG A-3'

(5) The multiple-base-mismatched target to P_{miR21} (miR-200b, T₄): 5'-UAA UAC UGC CUG GUA AUG AUG A-3'

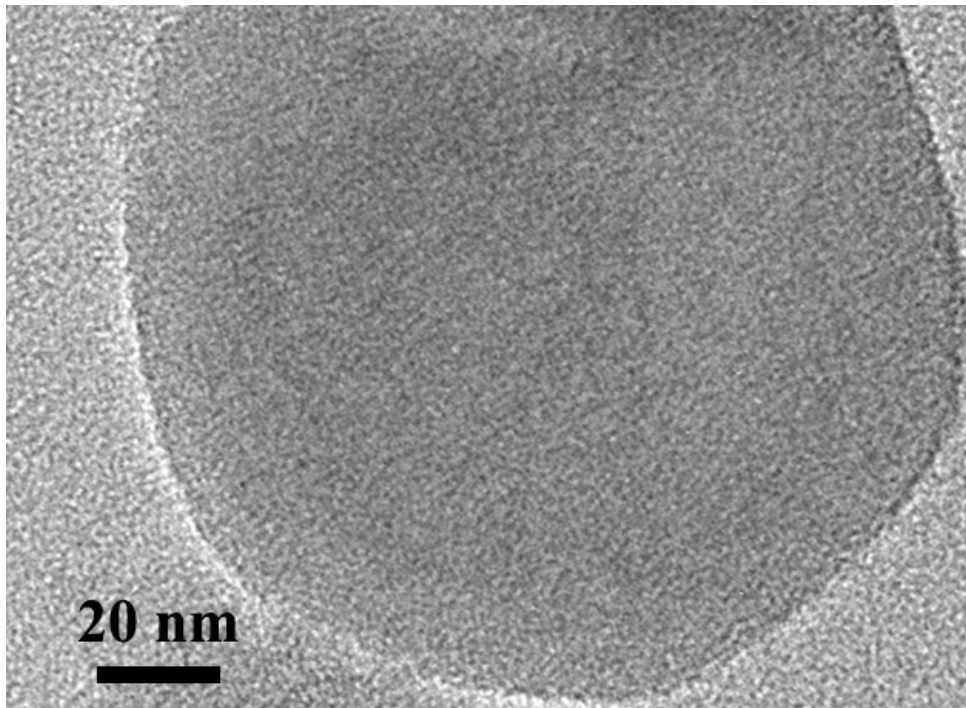


Fig. S1. Zoomed TEM image for h-BNNS.

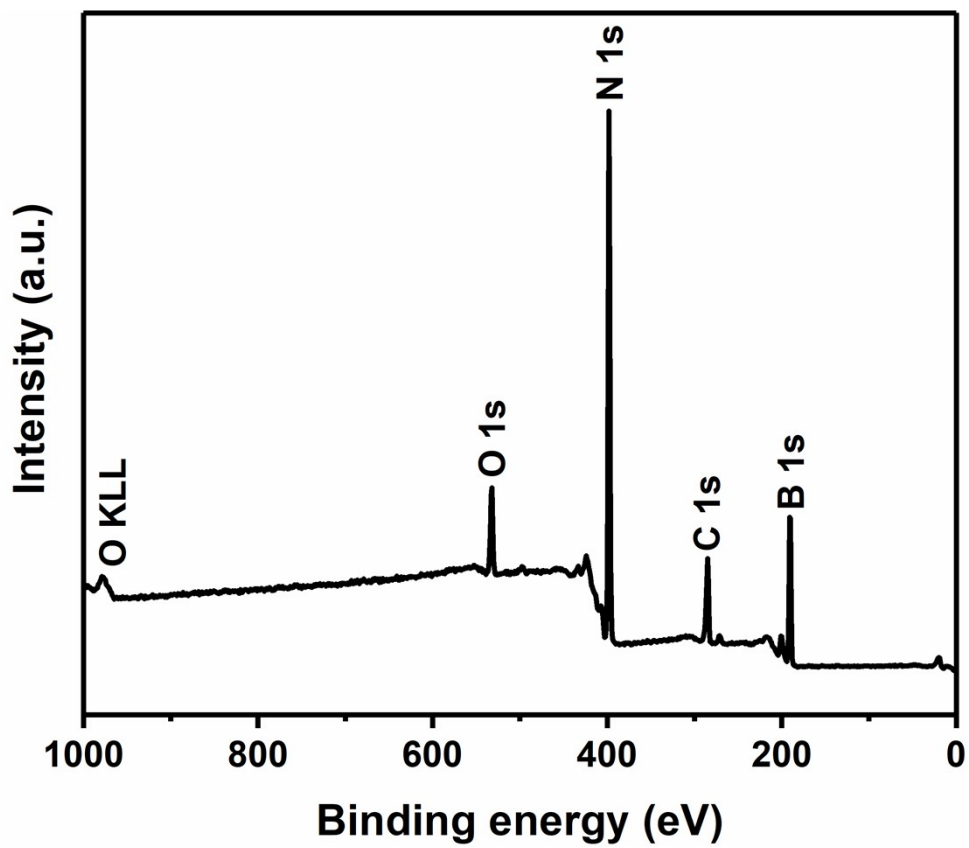


Fig. S2. XPS survey spectrum of h-BNNS.

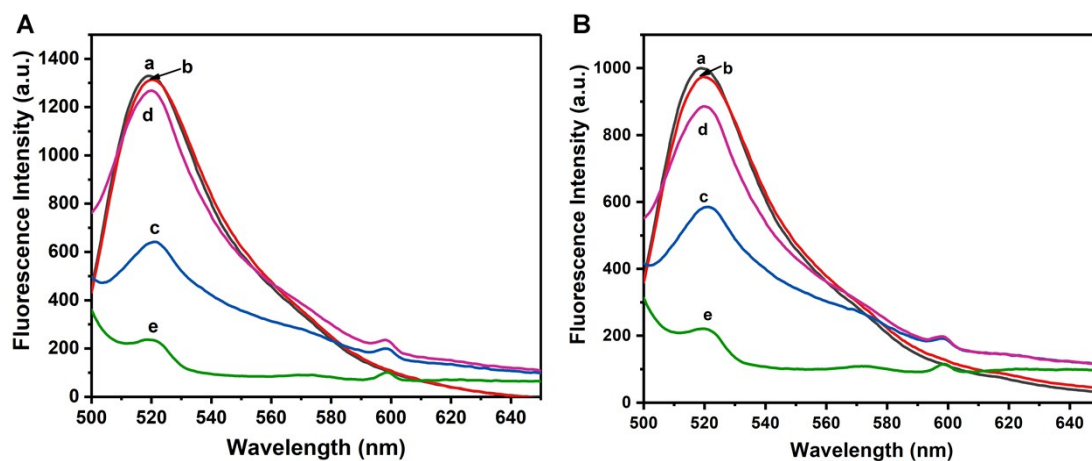


Fig. S3. (A) Fluorescence emission spectra of P_{miR21} at different conditions: a) P_{miR21} ; b) $P_{miR21} + T_1$; c) $P_{miR21} + h\text{-BNNS}$; d) $P_{miR21} + h\text{-BNNS} + T_1$; e) $h\text{-BNNS}$. (B) Fluorescence emission spectra of P_{miR21} at different conditions: a) P_{miR21} ; b) $P_{miR21} + T_1$; c) $P_{miR21} + h\text{-BN}$; d) $P_{miR21} + h\text{-BN} + T_1$; e) $h\text{-BN}$.

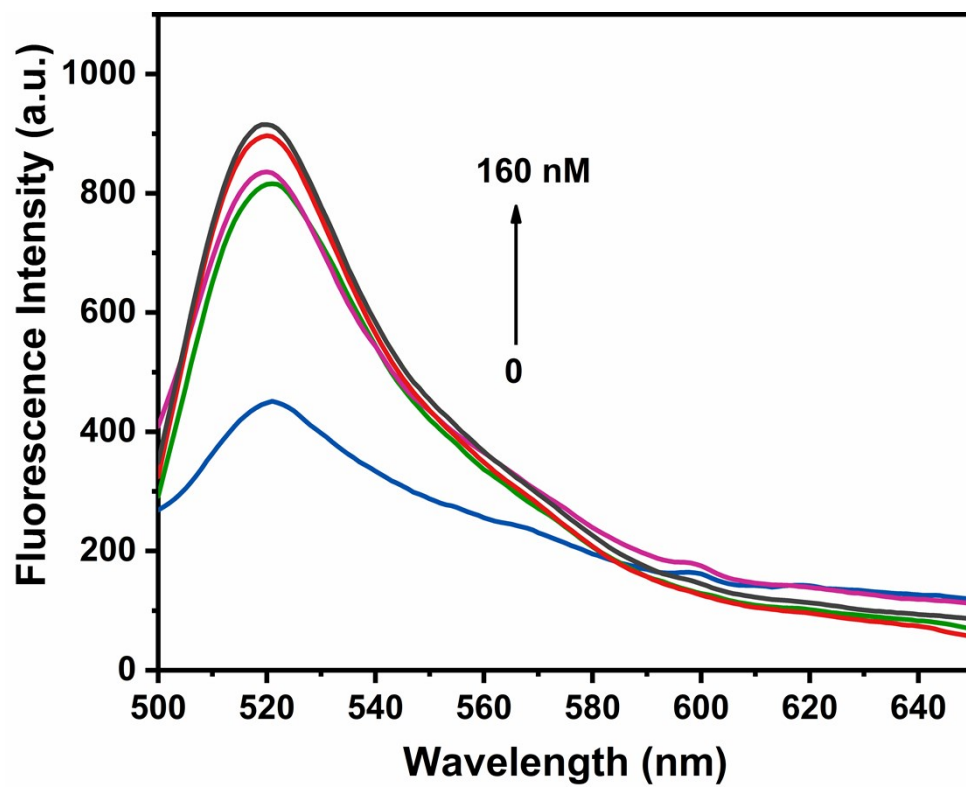


Fig. S4. Fluorescence intensity in the presence of the different concentrations of T₁ (blue line: 0 nM; green line: 20 nM; purple line: 40 nM; red line: 80 nM; black line: 160 nM.).

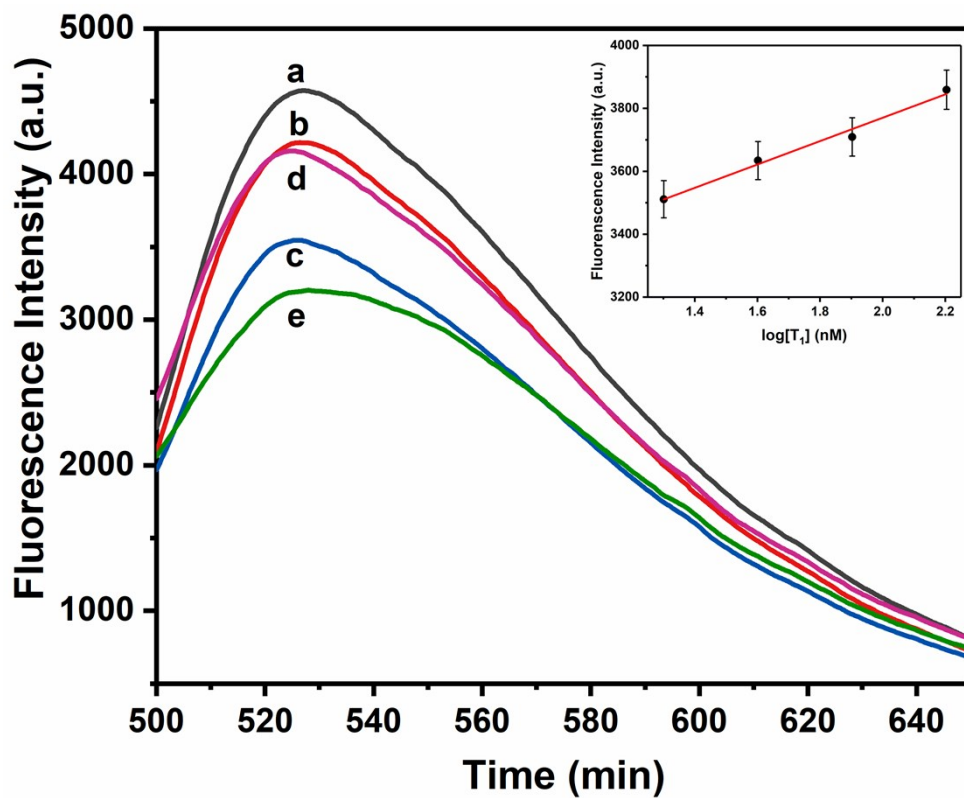


Fig. S5. Fluorescence emission spectra of P_{miR21} at different conditions in serum: a) P_{miR21} ; b) $P_{miR21} + T_1$; c) $P_{miR21} + h\text{-BNNS}$; d) $P_{miR21} + h\text{-BNNS} + T_1$; e) $h\text{-BNNS}$. Inset: the fluorescence intensity of $P_{miR21} + h\text{-BNNS}$ plotted against the logarithm of the concentration of T_1 .

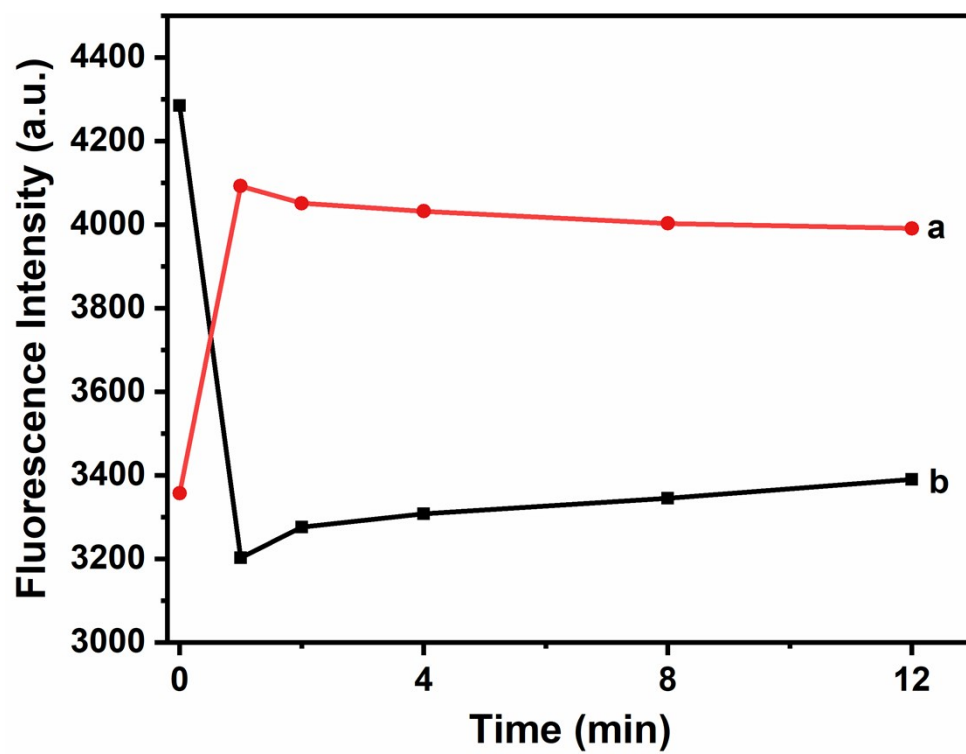


Fig. S6. Kinetic assays in serum: a) fluorescence recovery of $P_{\text{mir}21}$ -h-BNNS by T_1 , and b) fluorescence quenching of $P_{\text{mir}21}$ by h-BNNS.

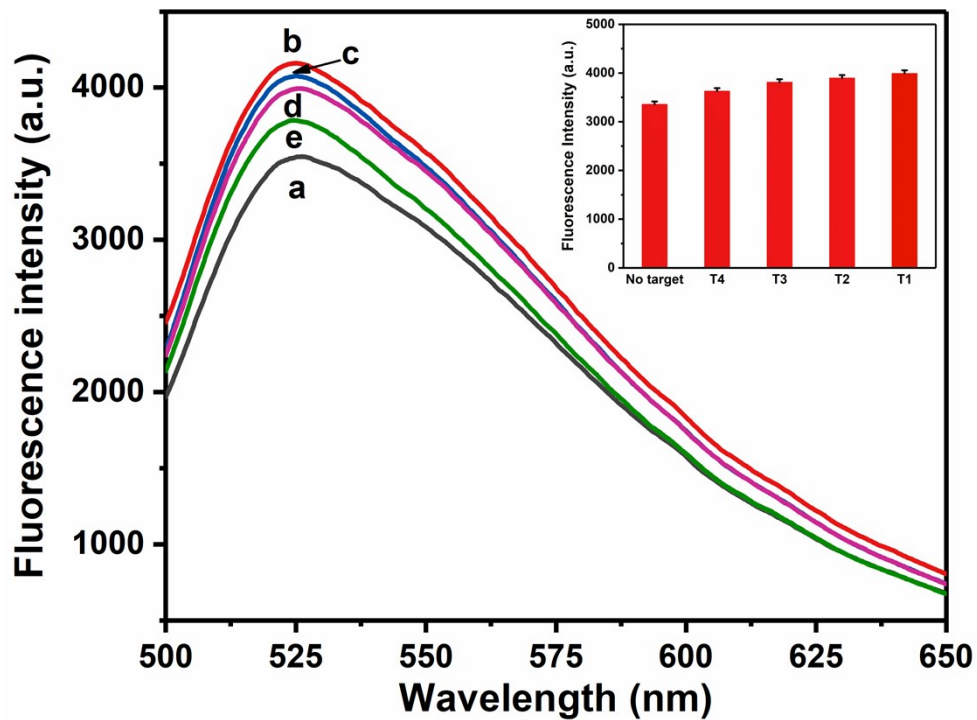


Fig. S7. Fluorescence emission spectra of P_{miR21} in the presence of h-BNNS at different conditions in serum: a) P_{miR21} -h-BNNS complex (background); b) P_{miR21} -h-BNNS complex + T₁; c) P_{miR21} -h-BNNS complex + T₂; d) P_{miR21} -h-BNNS complex + T₃; e) P_{miR21} -h-BNNS complex + T₄. Inset: the corresponding fluorescence intensity histograms with error bars.

Table S1. Comparison of the detection performances of h-BNNS with reported fluorescent miRNA detection platforms under the same fluorescence quenching mechanism.

Catalyst	Limit of detection	Ref.
h-BNNS	2.39 nM	This work
g-C ₃ N ₄	intracellular	1
RGO@PDA	11.29 nM	2
Carbon quantum dots	-	3

References

1. X. Liao, Q. Wang and H. Ju, *Chem. Commun.*, 2014, **50**, 13604-13607.
2. X. Li, T. Wang, Y. Luo, A. M. Asiri, S. Chen and X. Sun, *ChemBioChem*, 2020, **6**, 801-806.
3. F. Khakbaz and M. Mahani, *Anal. Biochem.*, 2017, **523**, 32-38.